# The role of membrane physiology in sHSP Lo18-lipid interaction and lipochaperone activity

Tiffany Bellanger, Frank Wien, Sophie Combet, Paloma Fernández Varela, Stéphanie Weidmann

# The role of membrane physiology in sHSP Lo18 -lipid interaction and lipochaperone activity

## Short Title: Lo18 membrane activity affected by lipid profiles

**Tiffany Bellanger[a], Frank Wien[b], Sophie Combet[c], Paloma Fernández Varela[d], Stéphanie Weidmann[a#]**

[a] Procédés Alimentaires et Microbiologiques (PAM), AgroSup Dijon, PAM UMR A 02.102, Laboratoire VAlMiS-IUVV, Dijon, France.

[#] Correspondence: stephanie.desroche@u-bourgogne.fr

[b]: Synchrotron SOLEIL, L'Orme des Merisiers, Saint Aubin BP 48, 91192, Gif-sur-Yvette, France

[c]: Laboratoire Léon-Brillouin (LLB), UMR12 CEA, CNRS, Université Paris-Saclay, F-91191, Gif-sur-Yvette CEDEX, France

[d]: Université Paris-Saclay, CEA, CNRS, Institute for Integrative Biology of the Cell (I2BC), 91198 Gif-sur-Yvette, France

**Abstract**

Lactic acid bacteria, such as *O. oeni*, face stress that affects membrane fluidity. To overcome this, small HSP are produced and act as chaperones and lipochaperones. However, the molecular mechanisms involved in lipochaperone activity are still poorly understood, particularly with regard to the influence of membrane lipid composition on this activity. This work aimed at characterizing the influence of the lipid environment and the physiological state of the membrane on the structure and lipochaperone activity of Lo18. In this context, liposomes derived from *O. oeni* cultures in exponential, stationary and adapted growth phases at 8% alcohol, representing the physiological states of unstressed, stressed and stress-adapted bacterial membranes, were produced and characterized. These liposomes were then used to observe the effect of the physiological state of the membranes on the lipochaperone activity and structural changes of Lo18. The results allowed us to identify the preferential affinity of Lo18 for lipids composed of oleic acid and/or phosphatidylglycerol, the mainly phospholipid component of the membranes not yet adapted to stress. The impact of this membrane composition on the structure, lipochaperone activity and the insertion of Lo18 into the different types of liposomes showed that: (i) the presence of the membrane (regardless of its nature) induces a modification of the structure of Lo18; (ii) the insertion of Lo18 into the membrane and/or the lipochaperone activity of Lo18 is enhanced when the membranes are rich in oleic acid and/or phosphatidylglycerol. This work contributes to a better understanding of interaction mechanisms between sHSPs and bacterial membranes.

## Introduction

The acidity and alcohol concentration present in wine are the main causes of membrane damage found in wine-grown cells [1]. Changes in the charge environment induced by low pH or -OH residues, which have a strong affinity for the polar heads of phospholipids, disrupt the organization and structure of the membrane, which has an impact on cell permeability and membrane fluidity [2, 3]. However, maintaining membrane fluidity is essential for the survival of

micro-organisms. Any change in membrane fluidity disrupts the flux of nutrients/wastes across the membrane and dissipates the proton motive force [4, 5], which can slow down cell metabolism, leading to cell growth arrest [6, 7]. Most of the key micro-organisms involved in the winemaking process have developed different strategies to maintain their membrane integrity.

For *Oenococcus oeni*, the main lactic acid bacteria involved in malolactic fermentation, one of these mechanisms is the synthesis of stress proteins, such as its unique small heat shock protein (sHSP) named Lo18. sHSPs are small proteins of 12 to 42 kDa, present in almost all organisms. In oligomeric state, they are mainly known for their ability to prevent the aggregation of cellular proteins owing to their chaperone activity [8–11]. However, for some sHSPs a second activity, known as molecular lipochaperone, has been described consisting in helping cells to maintain optimal membrane fluidity. Among these sHSPs are: HSPB1 and HSPB5 from humans [12], HSPA from *Synechococcus sp*. [10, 13], HSP17 from *Synechocystis sp*. [14, 15], HSP17.8 from *Arabidopsis thaliana* [16], HSP15.8 and HSP16 from *Schizosaccharomyces pombe* [17], HSP18.55 from *Lactiplantibacillus plantarum* [18] and Lo18 [11, 19–24]. According to the literature, when oligomers dissociate into dimers close to the membrane, electrostatic and hydrophobic forces deform the protein, allowing it to partially penetrate into the membrane and maintain optimal fluidity [25]. Regarding Lo18, previous studies have shown: (i) that the structure and oligomeric plasticity of the protein have an impact on lipochaperone activity [23, 24], and (ii) that Lo18 preferentially interacts with membrane lipids not yet adapted to stress [23]. However, the link between Lo18 lipochaperone activity, and more generally sHSPs, and the membrane lipid profile remains poorly described and understood.

The main aim of this study was to elucidate the links between the lipochaperone activity of Lo18 and the lipid composition and physical state of the membranes with which it interacts. First, the affinity of Lo18 for certain phospholipids constituting the membranes of *O. oeni* was investigated by immunolabelling, revealing a significant preference for lipids composed of phosphatidylglycerol and/or oleic acid. In parallel, the lipochaperone activity and structural changes of Lo18 were assessed during interaction with four types of liposomes representing the physiological states of unstressed, stressed and stress-adapted bacterial membranes. To do this, bacterial membranes from *O. oeni* from (i) exponential and stationary growth phase culture and (ii) 8% ethanol adapted culture were collected to create liposomes. The results showed that membrane interaction induced a change in the secondary structure of Lo18, characterized by an increase in α-helices at the expense of β-sheets for the liposomes tested. Additionally, the lipid composition of liposomes could influence the insertion of Lo18 into the membrane and lipochaperone activity.

## Results

### Favored lipidic Lo18 substrates

Over the last decade, a growing number of studies have focused on the lipochaperone activity of Lo18 [11, 20, 23, 24, 26]. However, to date, the lipid domains or lipids specifically involved in this interaction have not been identified. The affinity between Lo18 and several common phospholipids was analyzed by immunolabeling. The phospholipids were chosen for their presence in *O. oeni* membranes, and their physical properties. Regarding the physical properties, phospholipids were composed of: (i) either unsaturated (dioleoyl, DO-) or saturated (dipalmitoyl,

DP-) fatty acids, and (ii) neutral (phosphatidylethanolamine, -PE and phosphatidylcholine, -PC) or negative-charge head groups (phosphatidic acid, -PA and phosphatidylglycerol, -PG). The intensity of the signal obtained after hybridization with Lo18 was normalized with the quantity of phospholipids fixed on the PolyVinyliDene Fluoride (PVDF) membrane (obtained after staining with Nile Red) (Supplementary Data, Fig. S1). After this normalization step, Lo18 showed increased affinity for oleic acid (DOPG, DOPC and DOPE) and/or with the phosphatidylglycerol head group (DPPG and DOPG) (Fig. 1). The unsaturation present in the carbon chains of oleic acid naturally induces a certain disorder in the membrane, which is often observed in membranes not yet adapted to fluidifying stresses [27]. As described for HSP16 from *S. pombe* [17] and human HSPB1 [12, 28], this suggest Lo18 may preferentially interact with lipids found at the beginning of fluidification due to both hydrophobic and electrostatic interaction forces.

**Lipid membrane composition impacts Lo18 lipochaperone activity**

Given the affinity of Lo18 for certain phospholipids, it therefore seemed reasonable to examine whether the lipid composition and physiological state of membranes could have an impact on the lipochaperone activity of Lo18. To investigate this point, we used liposomes composed of purified lipids from cultures of *O. oeni* at different growth phases (exponential, stationary, and grown in the presence of 8% ethanol) representing the physiological states of unstressed, stressed and stress-adapted bacterial membranes, respectively. Liposomes composed of purified lipids from exponential *L. plantarum* cultures were also used as controls to test the specificity of Lo18 for lipids from its producer organism. The lipid composition of these four types of liposomes was first determined by chromatography (Fig. 2, Table S1). The results showed that digalactosyldiacylglycerols (DGDG) were the main head group found in *O. oeni* regardless of the growth phase, representing 38%, 64%, and 57% of the total head groups in liposomes from cultures in the exponential and stationary phases, or in the presence of 8% ethanol, respectively. For liposomes derived from the exponential phase culture of *O. oeni* and *L. plantarum*, phosphatidylglycerol (PG) represented a predominant head group, accounting for 39% of total lipids for *O. oeni* and 67% for *L. plantarum* (Fig. 1A, Table S1). Lysyl-PG, cardiolipins (CL) and phosphatidylcholins (PC) were also present in *O. oeni* and *L. plantarum* membranes in very low quantities, which could be considered as negligible. Regarding the fatty acid chains, they ranged from myristic acid, C14:0, to lactobacillic and dihydrosterulic acid (respectively cycC19:0 n-7 and cycC19:0 n-9), abbreviated C19:1 (Fig. 2B, Table S1). Palmitic acid, C16:0 (saturated), and oleic acid, C18:1 (unsaturated), were the most abundant fatty acids in *O. oeni* cells in the exponential and stationary phases in contrast with those present in *L. plantarum* cells, representing 37% and 26% in the exponential phase, 29% and 25% in the stationary phase, and 42% and 20% for the *L. plantarum* membrane respectively. During adaptation to alcohol the proportion of unsaturated fatty acids was significantly reduced, representing 12% of lipids compared with 28% and 29% in the exponential and stationary phases. This was mainly due to the decrease in the proportion of C18:1, from 26% in the exponential and 25% in the stationary phases to 11% in the presence of ethanol adapted membrane. Thus, by examining the nature of the polar heads and the fatty acid chains, four distinct profiles based on the prevalence of phosphatidylglycerol and oleic acid could be distinguished. It should be recalled that they are among the preferred lipid substrates of Lo18. Liposomes derived from *O. oeni* cultures in the exponential growth-phase are rich in PG and oleic acid (PG+, DO+), while those from the stationary phase are low in PG but rich in oleic acid (PG-, DO+). Liposomes derived from alcohol-adapted cultures were low in PG and oleic acid

(PG-, DO-), while those derived from a *L. plantarum* culture were high in PG but low in oleic acid (PG+, DO-).

The variation of the membrane fluidity of these four liposomes was then measured by steady-state fluorescence anisotropy of a 1,6-diphenyl-1,3,5-hexatriene probe (DPH) in the absence or presence of Lo18 during thermal ramping from 15 °C to 65 °C (Fig. 3, Table S2). The higher anisotropy means lower membrane fluidity. The ability of the Lo18 protein to maintain membrane fluidity was specific to the physiological state of the cells used to produced liposomes. Indeed, Lo18 maintained the membrane fluidity in liposomes from exponential growth phase cultures of both *O. oeni* and *L. plantarum*. From 45°C, fluidity reached 68% and 62% of their initial anisotropy value, respectively, in the presence of Lo18 versus 52%, and 56% in the absence of Lo18. Regarding liposomes from *O. oeni* culture in the stationary phase, the lipochaperone activity of Lo18 appeared later at 65°C. Finally, the lipochaperone activity of Lo18 over liposomes from ethanol-adapted *O. oeni* cultures was completely abolished in the temperature range 15°C to 65°C, where no difference was observed in the presence or absence of Lo18. However, it is important to take into account the difference in initial anisotropy, which is dependent on the lipid composition of the membranes used, and which may influence fluidization. This is particularly the case for membranes adapted to stress, which are more rigid.

**Impact of membrane lipid composition on the secondary structure of Lo18**

The modification of Lo18 lipochaperone activity linked to the physiological state of the membrane used was further characterized by investigating the modification of Lo18 secondary structures. To do this, Synchrotron radiation circular dichroism (SRCD) experiments were performed on Lo18 alone or in interaction with the four types of liposomes during thermal ramping from 20 °C to 60 °C. Along this ramp, 45° C, the temperature (Fig. 4A) corresponding to the temperature at which Lo18 starts its lipochaperone activity, is particularly interesting and will therefore be described in detail. At 45°C, the proportion of α-helixes increases significantly when Lo18 interacts with liposomes, starting at 3% for the protein alone to 6%, 8%, 24% and 6% in the presence of liposomes from *O. oeni* cells in the exponential and stationary phases, and ethanol-adapted cultures, respectively, as well as with *L. plantarum* cells (Figure 4). In contrast, the interaction with liposomes decreases the proportion of β-sheets. For Lo18 alone, the proportion of β-sheets was 42%, compared to 37%, 35%, 21%, and 31% upon interaction with liposomes from the exponential and stationary phases, the alcohol-adapted culture of *O. oeni*, and the culture of *L. plantarum,* respectively (Fig. 4). Thus, the presence of lipids modifies the structure of Lo18 more significantly than lipid composition.

In addition, the insertion of Lo18 into the different types of liposomes was also monitored by SRCD. This insertion was highlighted by a shift in the spectrum of polarized light towards the lower frequencies (bathochromic effect) when Lo18 was in the presence of certain liposomes. A clearly visualized shoulder (Fig 4B, in a rectangle box) appeared in the 195-210 nm range with liposomes derived from *O. oeni* cells in the exponential and stationary phases between 15 °C to 45°C. For example, at 15°C, the Δε value at 200 nm was -10.1 and -11.6 for these liposomes, respectively, compared to -14.7 for the protein alone. This shoulder was totally absent in the two otherconditions (-15.7 and -15.8 for liposomes derived from an alcohol-adapted culture and from a *L. plantarum* culture, respectively). Both these latter liposomes were the poorest in proportions of oleic acid in contrast to the liposomes from culture of *O. oeni* in exponential and stationary growth phases (Fig. 2). These differences in membrane composition, in particular the degree of fatty acid unsaturation, could influence membrane fluidity and also the distribution of

hydrophobic zones on the membrane surface. As Lo18 insertion is mainly observed in liposomes rich in oleic acid, it appears that this insertion can take place via hydrophobic interactions with relatively fluid membranes. The insertion could be observed up to 45°C (Fig. 4C), above which the structural change in Lo18 no longer allowed distinguishing this shoulder.

## Discussion

Membranes are the first cellular component affected by environmental changes. The viscosity of the membrane must remain close to 0.1 Pa.s. However, as a function of time and the intensity of the stresses encountered, this viscosity will be modified, leading the cells to adapt by fluidizing or rigidifying their membrane. [29]. To maintain optimum membrane fluidity, cells deploy a variety of mechanisms. In bacteria, adjustments such as changes in (i) saturated/unsaturated fatty acid ratios, (ii) the nature of unsaturation, (iii) the length of fatty acid carbon chains, or (iv) changes in polar heads are frequently observed [29–32]. However, these response mechanisms can only regulate membrane fluidity in the long term. To cope rapidly with an alteration in membrane integrity, cells have the capacity to synthesize proteins that regulate membrane fluidity, like sHSPs Lo18 synthetized by *O. oeni* [11, 20, 21, 23, 24].

Previous studies have shown that Lo18 has a stronger affinity for lipid substrates than for protein substrates; especially when the lipid composition of membranes is not yet adapted to stress. Until now, no specific affinities with phospholipids has been identified.[23]. In this context, the affinity between Lo18 and several phospholipids chosen for their physical properties was determined by immunolabeling. Although Lo18 interacts specifically with all the phospholipids tested, its affinity is most pronounced for lipids with a polar head group of PG and/ or oleic acid fatty acid chains. No interaction with DOPA was evidenced, certainly due to its conical conformation that might be less accessible [33]. Due to physical properties of PG and oleic acid, i.e. negatively charged and unsaturated fatty acids, respectively, the results suggest that Lo18 interacts via electrostatic and hydrophobic forces. These lipids are particularly represented in fluid membranes, classically found before lipid modification during adaptation to stress [29, 32, 34–36]. Indeed, both of these two phospholipid constituents are predominant in the membranes of both the exponential phase cultures (from *O. oeni* et *L. plantarum*) tested, mimicking unstressed membranes. This specific affinity for negatively charged lipids or fluid membranes has been reported for other sHSPs, such as human HSPB1 [12, 28], HSP16 from *S. pombe* [17], HSP17 from *Synechocystis* [37] and HSP12 from *Ustilago maydis* [38]. In all these cases, interaction appears to be mediated both by the state of fluidity of the membrane and by charges present at the lipid head and certain domains of the sHSP [12, 28]. More precisely, the hydrophobic domain of fatty acids could be used as an anchoring surface [28] and negative charges could attract the sHSPs on this surface.

To test the impact of these unsaturated (oleic acid) and negatively charged (PG) domains on Lo18/membrane interaction, Lo18 insertion into liposomes containing lipids from *O. oeni* or *L. plantarum* cultures at different physiological states (exponential growth, stationary phase or adaptation to 8% ethanol) was monitored by SRCD. The PG and oleic acid concentrations of these liposomes varied: rich in PG and oleic acid for membranes from *O. oeni* cultures in exponential phase, poor in PG and rich in oleic acid for those in stationary phase, poor in PG and oleic acid for those adapted to alcohol, and rich in PG but poor in oleic acid for membranes from *L. plantarum*

cultures in exponential phase (Figure 5A). A loss of negative absorption and a batho-chromic (red-) shift of the π-π*electronic transition at 208 nm translating protein insertion inability [39], were observed on SRCD spectra in the presence of ethanol-adapted liposomes and *L. plantarum* liposomes. Both these liposomes have the lowest content of oleic acids among the liposomes tested. This difference in fluidity mainly caused by the nature of the fatty acid chains, could change the insertion of Lo18 into the membrane as was observed for membrane proteins, human sHSPs such as HSPB1 and HSPB5 or HSP17 from *Synechocystis*, which insert more efficiently into liquid crystalline phase membranes than into gel phase membranes [12, 28, 38, 40–42]. Indeed, the more rigid the membrane, the less mobile and more ordered the phospholipids are, thereby reducing the efficiency of protein insertion [32]. The decrease of protein insertion due to greater bilayer stability may have an impact on protein activity, particularly lipochaperone activity, without necessarily abolishing it [43].

In addition to the impact on Lo18 insertion, the lipid composition of membrane could also impact the structure of the protein [43]. Indeed, a modification in membrane fluidity caused by the modification of the ratio between saturated/unsaturated fatty acids may also modify the attractive force around the membrane, leading to a modification of the secondary structure of Lo18. The secondary structure of Lo18 was determined during Lo18-liposome interaction by SRCD measurement. After interaction with the four types of liposomes at 45°C, an increase in the proportion of α-helices to the detriment of β-sheets was observed compared to the Lo18 protein alone. However, as this structural change occurred to a greater or lesser extent for all the liposomes tested, the presence of lipids (rather than their nature) was sufficient to cause the structural change in Lo18 [26, 44].

Both insertion and secondary structure modification due to membrane lipid composition may contribute to Lo18 lipochaperone activity [26]. Consequently, Lo18 lipochaperone activity was monitored during the fluidization of four different types of liposomes, two of which represent optimal growth conditions and the other two stress conditions. In the presence of liposomes mimicking *O. oeni* membranes adapted to stress (stationary phase and ethanol adapted, the lipochaperone activity of Lo18 was established at higher temperature or abolished. Furthermore, these stress-adapted liposomes had the lowest phosphatidylglycerol content, suggesting that the electrostatic attraction of proteins by the membrane may be a more significant factor than membrane fluidity in lipochaperone activity. Conversely, for Lo18 membrane insertion, membrane fluidity appeared to be an important factor.

Indeed, although Lo18 is unable to insert into liposomes extracted from a culture of *L. plantarum*, having a lipid profile (for the main polar heads) similar to that of *O. oeni* culture in exponential phase, it retains lipochaperone activity. It is therefore plausible that Lo18, like human sHSPs HSPB1 and HSPB5 [12] or HSP16 form *S. pombe* [17], may be attracted first by polar head groups before interacting with specific membrane microdomains [45] via an as yet unknown mechanism, allowing it to reinforce its lipochaperone activity.

The results obtained in this study lead us to propose a model. During membrane fluidization, dimers from cytoplasmic oligomeric structures (which regularly undergo association/dissociation cycles) are attracted to the membrane. Hydrophobic and electrostatic forces could attract them towards lipids, in particular unsaturated and negatively charged phospholipids (notably oleic acid and phosphatidylglycerol) for which Lo18 has greater affinity. In particular, it appears that the contribution of electrostatic forces induced by the polar heads

of membrane phospholipids may influence the lipochaperone activity of Lo18, whereas forces of a hydrophobic type would influence the insertion of Lo18 into membranes, which is consistent with current understanding of membrane protein insertion [40].(Fig. 5).

In conclusion, the present work contributes to a better understanding of the mechanisms of sHSPs and bacterial membrane interaction. Such understanding could allow the use the lipochaperone role of sHsps in different fields, such as in the agri-food industry, for example the resistance of *L. plantarum* to freeze drying processes [46] or in the medical field for the treatment of neurodegenerative diseases such as exudative retinopathy [47]

## Material and methods

### Media and growth conditions

*O. oeni* ATCC BAA-1163 was grown in modified FT80 medium [48] at pH 5.3 and 28 °C in the presence or absence of 8% ethanol. *L. plantarum* WFS1 was grown in MRS medium (Condalab, Spain) at pH 6.2 and 28 °C.

### Preparation of liposomes

*O. oeni* and *L. plantarum* cultures were grown to the exponential and/or stationary growth phase before lipids were extracted and purified according to Bligh and Dyer [49]. Liposomes were produced by adapting the method described by Maitre et al. 2012. [11]. The chloroform present in the lipid fraction was evaporated using a nitrogen flow. The lipids were then gently resuspended in 10 mL of 50 mM phosphate buffer, pH 7.0, previously heated to 55°C. After being sonicated twice for 2 min (Branson Ultrasonics™ CPX-952-138R, Branson Ultrasonics, Brookfield, CT, US), the lipid solution was rehydrated for 4 h at 55°C. The lipid particles were then extruded through a polycarbonate membrane with 1 µm-diameter pores to obtain the liposomes similar in size to *O. oeni* cells. The liposomes were stored at 4 °C for up to 1 week.

### Fluidity Measurements

Fluorescence anisotropy measurements (reflecting the fluidity state of the membrane) were performed using a FLUOROLOG-3 spectrofluorometer (Jobin Yvon Inc, USA). Each measurement was performed at excitation and emission wavelengths of 360 nm and 431 nm, respectively. Two hundred and fifty µL of liposomes and 3 µM of 1,6-diphenyl-1,3,5 hexatriene (DPH) probe (Sigma Aldrich, St. Louis, US) were mixed in a quartz cuvette (10 mm optical path) to a final volume of 3 mL. Measurements were performed on the liposome suspension in the presence or absence of Lo18 with a mass ratio of 1:2 (m/m) (Lo18/liposomes) following a temperature increase from 15 to 84 °C (2 °C *per* min increase) controlled by a Peltier system (QNW TC1 temperature controller, Quantum Northwest, Liberty Lake, WA, USA). For each experiment, an anisotropy value was obtained every 14.6 s and calculated according to Shinitzky and Barenholz 1978[50]. Each experiment was performed in triplicate.

### Synchrotron radiation circular dichroism (SRCD) spectroscopy

Circular dichroism spectra were collected on the DISCO beamline (Synchrotron SOLEIL, France) according to [51]. The instrument was calibrated using 99% pure (+) camphor-10-sulphonic acid (Sigma Aldrich, Saint-Louis, US) at 25 °C after each beam fill [52]. Lo18 at 140 µM was prepared in 50 mM sodium phosphate buffer, pH 7.0, alone or in the presence of liposomes at 250 µM. Then, 50 µL of sample was loaded into a 0.02 cm pathlength demountable cylindrical Suprasil quartz cell (Hellma, Germany) and subjected to a thermal scan from 15 °C to 84 °C with a step of

3 °C. Each dataset was collected from 262 nm to 176 nm, with an integration time of 1.2 s and a spectral bandwidth of 1 nm. Three scans of each sample and the equivalent baseline were collected. The sample spectrum was averaged across the three repeats, and the averaged baselines (buffer without protein) subtracted. Baseline-subtracted spectra were zeroed between 250 and 260 nm. All the spectra were normalized according to the protein concentration and pathlength using the CDToolX software and deconvoluted using BeStSel online software [53].

### Lipid Protein overlay assay

The interactions between lipids and Lo18 or modified proteins were observed by immunostaining, according to [54]. A drop of 2 µL of dipalmitoyl phosphatidylethanolamine (DPPE), dioleoyl phosphatidylethanolamine (DOPE), dioleoyl phosphatidic acid (DOPA), dipalmitoyl phosphatidylcholine (DPPC), dioleoyl phosphatidylcholine (DOPC), dipalmitoyl phosphatidylglycerol (DPPG), and dioleoylphosphatidylglycerol (DOPG) (Avanti polar, France) at 1.5 mM was deposited on a PVDF membrane (Fisher scientific, USA). The membrane was blocked in TBS/Regilait 5%, 1 h at 70 rpm and washed three times for 5 min with TBS. It was then incubated with Lo18 or modified purified protein at 7.5 µg/mL and washed again three times. Afterward, the protein bound to the lipids was detected with antibodies against Lo18 (1/750), produced by Eurogenetec with mice, and against the primary antibody (1/2000) against mice antibodies by incubating the membrane for 1 h at 70 rpm for each antibody. Chemiluminescence was detected using the ECL reagent kit (Thermo Fisher, USA). A normalization step was added to quantify the interaction between Lo18 and the phospholipids. To do this, the proportion of phospholipids fixed to the PVDF membrane was measured by fluorescence imaging after 15 min incubation with 50 mM of Nile Red staining. Then the signal intensity obtained for the immunolabeling measurement was adjusted to the signal obtained for the Nile Red staining.

## Lipidomic analysis

### Total fatty acids analysis by GCMS-NCI

Bligh and Dyer lipid extracts (50 µL) were mixed with 25 µL of a fatty acid internal standard mix (Avanti Polar Lipids, France) containing: 1146 ng of myristic acid-d3, 4973 ng of palmitic acid-d3, 3703 ng of stearic acid-d3, 3174 ng of linoleic acid d4, 45.8 ng of arachidic acid-d3, 1632 ng of arachidonic acid-d8, 47.6 ng of behenic acid-d3, 476.1 ng of DHA-d5, 22.9 ng of Lignoceric-d4, and 17.6 ng of cerotic acid-d4. Total fatty acids were quantitated after alkaline hydrolysis by GCMS-NCI, as previously described [55]

### Lipid analysis by LCMS2

Bligh and Dyer lipid extracts (200 µL) were dried under vacuum and mixed with an internal standard mix (50 µL) (CDN Isotopes, France and Cayman, France), (14:0)4CL (800 ng), (12:0)2DG (8 µg), and (21:0)2PC (50 ng). Sample (1 µL) was analyzed by LCMSMS using a Zorbax®Eclipse Plus C18 1.8 µm, 2.1 x 100 mm column maintained at 55 °C (Agilent Technologies).

Briefly, digalactosyldiacylglycerols (DGDG), monogalactosyldiacylglycerols (MGDG), and diacylglycerols (DG) were separated on a 1260 Infinity LC system (Agilent Technologies) with a gradient of mobile phase A (acetonitrile/water/1M ammonium formate (60/39/1 v/v/v) with 0.1% formic acid), and mobile phase B (isopropanol/acetonitrile/1M ammonium formate (90/9/1 v/v/v) with 0.1% formic acid) [56] at a flow rate of 0.4 mLmL/min set as follows: 1 min hold at 50% B; 50-60% B in 4 min; 60-85% B in 10 min; 85-99% B in 1 min; 2 min hold at 99%, 99%-50% ramp-down in 0.1 min and maintained at 50% B for 3.9 min. Acquisition was carried out on a 6460 Triple

Quadrupole (Agilent Technologies) equipped with an ESI Jet stream source (temperature 250 °C, nebulizer 20 L/min, sheath gas 11 L/min, sheath gas temperature 220 °C, capillary 3500 V, nozzle 1000 V) operating in positive Single Reaction Monitoring (SRM) mode (fragmentor 148 V, collision energy 23 V). Transitions were set as the neutral loss of 359 Da for DGDG or 197 Da for MGDG from their respective [M+NH4]+ ions [57] DG (as NH4+ adducts) were quantified according to the sum of the signal resulting from the neutral loss of either their sn-1 or sn-2 fatty acid. Finally, lipid concentrations were determined by calculating their relative response to (12:0)2DG used as internal standard.

Phosphatidylglycerols (PG) and lysyl-phosphatidylglycerols (lysyl-PG) were separated with the same mobile phases and column as for DGs, and the elution gradient used was set as follows: 2 min hold at 50% B; 50-99% B in 14 min; 2 min hold at 99%, 99%-50% ramp-down in 0.1 min; return to initial conditions in 1.9 min. Acquisition was carried out on a 6460 Triple Quadrupole (Agilent Technologies) equipped with an ESI Jet stream source (temperature 200 °C, nebulizer 20 L/min, sheath gas 11 L/min, sheath gas temperature 220 °C, capillary 3500 V, nozzle 1000 V) operating in positive Single Reaction Monitoring (SRM) mode (fragmentor/collector 116 V/13 V and 300 V/34 V for PG and Lysyl-PG respectively). Transitions were set as the neutral loss of 189 Da or 300 Da for [PG+NH4]+ and [Lysyl-PG+H]+ ions respectively. Lipid concentrations were determined by calculating relative response ratios with regards to (12:0)2DG used as internal standard.

The analysis of cardiolipins (CL) and phosphatidylcholines (PC) was performed as previously described [58, 59] except that a Vanquish LC system, coupled to a triple-stage quadrupole (TSQ) Altis mass spectrometer equipped with a heated electrospray ionization source (Thermo Scientific) was used (sheath gas, 50 arb; auxiliary gas, 10 arb; sweep gas, 1 arb; ion transfer tube temperature, 325 °C; vaporizer tempropylerature, 350 °C and ion spray voltage, 3500 V (+), and 2500 V (-)). Lipid concentrations for all the quantified lipid classes were expressed in pmol/mg of Bligh and Dyer extract.

### Statistical analysis

For each condition tested on fluorescence anisotropy, immunolabelling, lipidic profile, and secondary structure analysis were performed using three independent measurements. The anisotropy values obtained were normalized to be expressed in percentage compared to the initial value at 15 °C. Statistical analyses were performed by the statistical RStudio software (version 1.2.5033). The normality of the distribution and homogeneity of the variances of each condition were tested by the Shapiro-Wilk test and the Bartlett test, respectively. Then, a non-parametric Kruskal-Wallis test was used to compare the samples with a significance level of $\alpha = 0.05$. All the statistical tests were considered significant at a p-value $<0.05$.

**Acknowledgments**

The present work was supported by the Regional Council of Bourgogne- Franche-Comté Bourgogne grant number 2021Y-09559, and the Ministère de l'Enseignement supérieur, de la Recherche et de l'Innovation, grant number MESR 2020–04. The authors would like to thank the Dimacell Platform (Agrosup Dijon, INRA, INSERM, Univ. Bourgogne Franche-Comté, F-21000 Dijon France), the lipidomic platform (LAP, Université de Bourgogne, Dijon, France), and the Synchrotron SOLEIL (Saint-Aubin, France) for X-ray beamtime on the DISCO beamline (project #20220067). We would also like to thank Accent Europe for proofreading the English text.

**Conflicts of Interest:** The authors declare no conflict of interest.

**Author contribution: T. B.** and **S. W**: Conceptualization, T. **B.,** and **S. W:** Methodology, **T. B.** Formal analysis, **T. B.and S. W.:** Investigation, **T. B., S. W and F. W.:** Resources, **T. B.** and **S. W** : Writing – Original Draft, **T.B, S. W., F. W., , P. F.-V.** and **S. C**. : Writing – Review & Editing; **S. W.**: Validation, Project administration and Funding acquisition

**Data avaibility:** The datasets generated during and/or analysed during the current study are available from the corresponding author on reasonable request.

**References:**


1 Chu-Ky, S., Tourdot-Marechal, R., Marechal, P.-A. and Guzzo, J. (2005) Combined cold, acid, ethanol shocks in *Oenococcus oeni*: Effects on membrane fluidity and cell viability. *Biochimica et Biophysica Acta (BBA) - Biomembranes* **1717**, 118–124 https://doi.org/10.1016/j.bbamem.2005.09.015

2 Da Silveira, M. G., Golovina, E. A., Hoekstra, F. A., Rombouts, F. M. and Abee, T. (2003) Membrane fluidity adjustments in ethanol-stressed *Oenococcus oeni* cells. *AEM* **69**, 5826–5832 https://doi.org/10.1128/AEM.69.10.5826-5832.2003

3 Wen-ying, Z. and Zhen-kui, K. (2013) Advanced progress on adaptive stress response of *Oenococcus oeni*. *Journal of Northeast Agricultural University (English Edition)* **20**, 91–96 https://doi.org/10.1016/S1006-8104(13)60015-X

4 D'Amico, S., Collins, T., Marx, J., Feller, G., Gerday, C. and Gerday, C. (2006) Psychrophilic microorganisms: challenges for life. *EMBO Rep* **7**, 385–389 https://doi.org/10.1038/sj.embor.7400662

5 Olguín, N., Bordons, A. and Reguant, C. (2009) Influence of ethanol and pH on the gene expression of the citrate pathway in *Oenococcus oeni*. *Food Microbiology* **26**, 197–203 https://doi.org/10.1016/j.fm.2008.09.004

6 Cisilotto, B., Scariot, F. J., Vivian Schwarz, L., Mattos Rocha, R. K., Longaray Delamare, A. P. and Echeverrigaray, S. (2021) Yeast stress and death caused by the synergistic effect of ethanol and $SO^2$ during the second fermentation of sparkling wines. *OENO One* **55**, 49–69 https://doi.org/10.20870/oeno-one.2021.55.4.4809

7 Gonzalez, R. and Morales, P. (2022) Truth in wine yeast. *Microbial Biotechnology* **15**, 1339–1356 https://doi.org/10.1111/1751-7915.13848

8 Mogk, A., Ruger-Herreros, C. and Bukau, B. (2019) Cellular functions and mechanisms of action of small heat shock proteins. *Annu. Rev. Microbiol.* **73**, 89–110 https://doi.org/10.1146/annurev-micro-020518-115515

9 Haslbeck, M. and Vierling, E. (2015) A first line of stress defense: small heat shock proteins and their function in protein homeostasis. *Journal of Molecular Biology* **427**, 1537–1548 https://doi.org/10.1016/j.jmb.2015.02.002

10 Obuchowski, I. and Liberek, K. (2020) Small but mighty: a functional look at bacterial sHSPs. *Cell Stress and Chaperones* **25**, 593–600 https://doi.org/10.1007/s12192-020-01094-0

11 Maitre, M., Weidmann, S., Rieu, A., Fenel, D., Schoehn, G., Ebel, C., et al. (2012) The oligomer plasticity of the small heat-shock protein Lo18 from *Oenococcus oeni* influences its role in both membrane stabilization and protein protection. *Biochemical Journal* **444**, 97–104 https://doi.org/10.1042/BJ20120066

12 De Maio, A., Cauvi, D. M., Capone, R., Bello, I., Egberts, W. V., Arispe, N., et al. (2019) The small heat shock proteins, HSPB1 and HSPB5, interact differently with lipid membranes. *Cell Stress and Chaperones* **24**, 947–956 https://doi.org/10.1007/s12192-019-01021-y

13 Nitta, K., Suzuki, N., Honma, D., Kaneko, Y. and Nakamoto, H. (2005) Ultrastructural stability under high temperature or intensive light stress conferred by a small heat shock protein in cyanobacteria. *FEBS Letters* **579**, 1235–1242 https://doi.org/10.1016/j.febslet.2004.12.095

14 Török, Z., Goloubinoff, P., Horváth, I., Tsvetkova, N. M., Glatz, A., Balogh, G., et al. (2001) *Synechocystis* HSP17 is an amphitropic protein that stabilizes heat-stressed membranes and binds denatured proteins for subsequent chaperone-mediated refolding. *Proceedings of the National Academy of Sciences* **98**, 3098–3103 https://doi.org/10.1073/pnas.051619498
15 De Maio, A. and Hightower, L. E. (2021) Heat shock proteins and the biogenesis of cellular membranes. *Cell Stress and Chaperones* **26**, 15–18 https://doi.org/10.1007/s12192-020-01173-2
16 Kim, D. H., Xu, Z.-Y., Na, Y. J., Yoo, Y.-J., Lee, J., Sohn, E.-J., et al. (2011) Small heat shock protein Hsp17.8 functions as an Akr2a cofactor in the targeting of chloroplast outer membrane proteins in arabidopsis. *Plant Physiology* **157**, 132–146 https://doi.org/10.1104/pp.111.178681
17 Glatz, A., Pilbat, A.-M., Németh, G. L., Vince-Kontár, K., Jósvay, K., Hunya, Á., et al. (2016) Involvement of small heat shock proteins, trehalose, and lipids in the thermal stress management in *Schizosaccharomyces pombe*. *Cell Stress and Chaperones* **21**, 327–338 https://doi.org/10.1007/s12192-015-0662-4
18 Rocchetti, M. T., Bellanger, T., Trecca, M. I., Weidmann, S., Scrima, R., Spano, G., et al. (2023) Molecular chaperone function of three small heat-shock proteins from a model probiotic species. *Cell Stress and Chaperones* **28**, 79–89 https://doi.org/10.1007/s12192-022-01309-6
19 Delmas, F., Pierre, F., Divies, C. and Guzzo, J. (2001) Biochemical and physiological studies of the small heat shock protein Lo18 from the lactic acid bacterium *Oenococcus oeni*. *Journal of molecular microbiology and biotechnology* **3**, 601–610
20 Coucheney, F., Gal, L., Beney, L., Lherminier, J., Gervais, P. and Guzzo, J. (2005) A small HSP, Lo18, interacts with the cell membrane and modulates lipid physical state under heat shock conditions in a lactic acid bacterium. *Biochimica et Biophysica Acta (BBA) - Biomembranes* **1720**, 92–98 https://doi.org/10.1016/j.bbamem.2005.11.017
21 Jobin, M.-P., Delmas, F., Garmyn, D., Diviès, C. and Guzzo, J. (1997) Molecular characterization of the gene encoding an 18-kilodalton small heat shock protein associated with the membrane of *Leuconostoc oenos*. *Applied and environmental microbiology* **63**, 609–614 https://doi.org/10.1128/AEM.63.2.609-614.1997
22 Guzzo, J., Delmas, F., Pierre, F., Jobin, M.-P., Samyn, B., Van Beeumen, J., et al. (1997) A small heat shock protein from *Leuconostoc oenos* induced by multiple stresses and during stationary growth phase. *Letters in Applied Microbiology* **24**, 393–396 https://doi.org/10.1046/j.1472-765X.1997.00042.x
23 Maitre, M., Weidmann, S., Dubois-Brissonnet, F., David, V., Covès, J. and Guzzo, J. (2014) Adaptation of the wine bacterium *Oenococcus oeni* to ethanol stress: role of the small heat shock protein Lo18 in membrane integrity. *Appl. Environ. Microbiol.* (Pettinari, M. J., ed.) **80**, 2973–2980 https://doi.org/10.1128/AEM.04178-13
24 Weidmann, S., Rieu, A., Rega, M., Coucheney, F. and Guzzo, J. (2010) Distinct amino acids of the *Oenococcus oeni* small heat shock protein Lo18 are essential for damaged protein protection and membrane stabilization: Protein protection and membrane stabilization by smHsp Lo18. *FEMS Microbiology Letters* no-no https://doi.org/10.1111/j.1574-6968.2010.01999.x
25 Bellanger, T. and Weidmann, S. (2023) Is the lipochaperone activity of sHSP a key to the stress response encoded in its primary sequence? *Cell Stress and Chaperones* **28**, 21–33 https://doi.org/10.1007/s12192-022-01308-7
26 Bellanger, T., da Silva Barreira, D., Wien, F., Delarue, P., Senet, P., Rieu, A., et al. (2023) Significant influence of four highly conserved amino-acids in lipochaperon-active sHsps on the structure and functions of the Lo18 protein. *Sci Rep* **13**, 19036 https://doi.org/10.1038/s41598-023-46306-6

27 O'Leary, W. M. (1962) THE FATTY ACIDS OF BACTERIA. *Bacteriol Rev* **26**, 421–447 https://doi.org/10.1128/br.26.4.421-447.1962
28 Csoboz, B., Gombos, I., Kóta, Z., Dukic, B., Klement, É., Varga-Zsíros, V., et al. (2022) The small heat shock protein, HSPB1, interacts with and modulates the physical structure of membranes. *IJMS* **23**, 7317 https://doi.org/10.3390/ijms23137317
29 Denich, T. J., Beaudette, L. A., Lee, H. and Trevors, J. T. (2003) Effect of selected environmental and physico-chemical factors on bacterial cytoplasmic membranes. *Journal of Microbiological Methods* **52**, 149–182 https://doi.org/10.1016/S0167-7012(02)00155-0
30 Beney, L. and Gervais, P. (2001) Influence of the fluidity of the membrane on the response of microorganisms to environmental stresses. *Applied Microbiology and Biotechnology* **57**, 34–42 https://doi.org/10.1007/s002530100754
31 Bouix, M. and Ghorbal, S. (2015) Rapid assessment of *Oenococcus oeni* activity by measuring intracellular pH and membrane potential by flow cytometry, and its application to the more effective control of malolactic fermentation. *International Journal of Food Microbiology* **193**, 139–146 https://doi.org/10.1016/j.ijfoodmicro.2014.10.019
32 Fonseca, F., Pénicaud, C., Tymczyszyn, E. E., Gómez-Zavaglia, A. and Passot, S. (2019) Factors influencing the membrane fluidity and the impact on production of lactic acid bacteria starters. *Appl Microbiol Biotechnol* **103**, 6867–6883 https://doi.org/10.1007/s00253-019-10002-1
33 Zhukovsky, M. A., Filograna, A., Luini, A., Corda, D. and Valente, C. (2019) Phosphatidic acid in membrane rearrangements. *FEBS Letters* **593**, 2428–2451 https://doi.org/10.1002/1873-3468.13563
34 Grogan, D. W. and Cronan, J. E. (1997) Cyclopropane ring formation in membrane lipids of bacteria. *Microbiology and Molecular Biology Reviews*, American Society for Microbiology **61**, 429–441 https://doi.org/10.1128/mmbr.61.4.429-441.1997
35 Bouix, M. and Ghorbal, S. (2017) Assessment of bacterial membrane fluidity by flow cytometry. *Journal of Microbiological Methods* **143**, 50–57 https://doi.org/10.1016/j.mimet.2017.10.005
36 Cronan, J. E. (2002) Phospholipid modifications in bacteria. *Current Opinion in Microbiology* **5**, 202–205 https://doi.org/10.1016/S1369-5274(02)00297-7
37 Tsvetkova, N. M., Horvath, I., Torok, Z., Wolkers, W. F., Balogi, Z., Shigapova, N., et al. (2002) Small heat-shock proteins regulate membrane lipid polymorphism. *Proceedings of the National Academy of Sciences* **99**, 13504–13509 https://doi.org/10.1073/pnas.192468399
38 Mitra, A., Bhakta, K., Kar, A., Roy, A., Mohid, S. A., Ghosh, A., et al. (2023) Insight into the biochemical and cell biological function of an intrinsically unstructured heat shock protein, Hsp12 of Ustilago maydis. *Molecular Plant Pathology* **24**, 1063–1077 https://doi.org/10.1111/mpp.13350
39 Bürck, J., Wadhwani, P., Fanghänel, S. and Ulrich, A. S. (2016) Oriented circular dichroism: a method to characterize membrane-active peptides in oriented lipid bilayers. *Acc. Chem. Res.* **49**, 184–192 https://doi.org/10.1021/acs.accounts.5b00346
40 Davletov, B., Perisic, O. and Williams, R. L. (1998) Calcium-dependent Membrane Penetration Is a Hallmark of the C2 Domain of Cytosolic Phospholipase A2 Whereas the C2A Domain of Synaptotagmin Binds Membranes Electrostatically. *Journal of Biological Chemistry* **273**, 19093–19096 https://doi.org/10.1074/jbc.273.30.19093
41 Balogi, Z., Cheregi, O., Giese, K. C., Juhász, K., Vierling, E., Vass, I., et al. (2008) A mutant small heat shock protein with increased thylakoid association provides an elevated resistance against UV-B Damage in Synechocystis 6803. *Journal of Biological Chemistry* **283**, 22983–22991 https://doi.org/10.1074/jbc.M710400200
42 Horváth, I., Multhoff, G., Sonnleitner, A. and Vígh, L. (2008) Membrane-associated stress proteins: More than simply chaperones. *Biochimica et Biophysica Acta (BBA) - Biomembranes* **1778**, 1653–1664 https://doi.org/10.1016/j.bbamem.2008.02.012

43 Lenaz, G. (1987) Lipid fluidity and membrane protein dynamics. *Bioscience Reports* **7**, 823–837 https://doi.org/10.1007/BF01119473

44 Balogi, Z., Török, Z., Balogh, G., Jósvay, K., Shigapova, N., Vierling, E., et al. (2005) "Heat shock lipid" in cyanobacteria during heat/light-acclimation. *Archives of Biochemistry and Biophysics* **436**, 346–354 https://doi.org/10.1016/j.abb.2005.02.018

45 Nickels, J. D., Hogg, J., Cordner, D. and Katsaras, J. (2020) Lipid rafts in bacteria: structure and function. in health consequences of microbial interactions with hydrocarbons, oils, and lipids (Goldfine, H., ed.), pp 3–32, Springer International Publishing, Cham https://doi.org/10.1007/978-3-030-15147-8_3

46 Arena, M. P., Capozzi, V., Longo, A., Russo, P., Weidmann, S., Rieu, A., et al. (2019) The phenotypic analysis of *Lactobacillus plantarum* sHSP mutants reveals a potential role for hsp1 in cryotolerance. *Front. Microbiol.* **10**, 838 https://doi.org/10.3389/fmicb.2019.00838

47 Tóth, M. E., Sántha, M., Penke, B. and Vígh, L. (2015) How to stabilize both the proteins and the membranes: diverse effects of shsps in neuroprotection. in the big book on Small Heat Shock Proteins (Tanguay, R. M., and Hightower, L. E., eds.), pp 527–562, Springer International Publishing, Cham https://doi.org/10.1007/978-3-319-16077-1_23

48 Cavin, J. F., Prevost, H., Lin, J., Schmitt, P. and Divies, C. (1989) Medium for Screening *Leuconostoc oenos* Strains Defective in Malolactic Fermentation. *Appl Environ Microbiol* **55**, 751–753

49 Bligh, E. G. and Dyer, W. J. (1959) A rapid method of total lipid extraction and purification - PubMed. *Canadian journal of biochemistry and physiology* **37**, 911–917

50 Shinitzky, M. and Barenholz, Y. (1978) Fluidity parameters of lipid regions determined by fluorescence polarization. *Biochimica et Biophysica Acta (BBA) - Reviews on Biomembranes* **515**, 367–394 https://doi.org/10.1016/0304-4157(78)90010-2

51 Evans, P., Wyatt, K., Wistow, G. J., Bateman, O. A., Wallace, B. A. and Slingsby, C. (2004) The P23T cataract mutation causes loss of solubility of folded γD-Crystallin. *Journal of Molecular Biology* **343**, 435–444 https://doi.org/10.1016/j.jmb.2004.08.050

52 Miles, A. J., Wien, F. and Wallace, B. A. (2004) Redetermination of the extinction coefficient of camphor-10-sulfonic acid, a calibration standard for circular dichroism spectroscopy. *Anal Biochem* **335**, 338–339 https://doi.org/10.1016/j.ab.2004.08.035

53 Micsonai, A., Moussong, É., Wien, F., Boros, E., Vadászi, H., Murvai, N., et al. (2022) BeStSel: webserver for secondary structure and fold prediction for protein CD spectroscopy. *Nucleic Acids Res* **50**, W90–W98 https://doi.org/10.1093/nar/gkac345

54 Dowler, S., Kular, G. and Alessi, D. R. (2002) Protein Lipid Overlay Assay. *Science Signaling* 11 https://doi.org/10.1126/stke.2002.129.pl6

55 Blondelle, J., Pais De Barros, J.-P., Pilot-Storck, F. and Tiret, L. (2017) Targeted lipidomic analysis of myoblasts by GC-MS and LC-MS/MS. In Skeletal Muscle Development (Ryall, J. G., ed.), pp 39–60, Springer New York, New York, NY https://doi.org/10.1007/978-1-4939-7283-8_4

56 Cajka, T., Hricko, J., Rudl Kulhava, L., Paucova, M., Novakova, M. and Kuda, O. (2023) Optimization of mobile phase modifiers for fast lc-ms-based untargeted metabolomics and lipidomics. *IJMS* **24**, 1987 https://doi.org/10.3390/ijms24031987

57 Carriot, N., Paix, B., Greff, S., Viguier, B., Briand, J.-F. and Culioli, G. (2021) Integration of LC/MS-based molecular networking and classical phytochemical approach allows in-depth annotation of the metabolome of non-model organisms - The case study of the brown seaweed Taonia atomaria. *Talanta* **225**, 121925 https://doi.org/10.1016/j.talanta.2020.121925

58 Vial, G., Chauvin, M.-A., Bendridi, N., Durand, A., Meugnier, E., Madec, A.-M., et al. (2015) Imeglimin Normalizes glucose tolerance and insulin sensitivity and improves mitochondrial function in liver of a high-fat, high-sucrose diet mice model. *Diabetes* **64**, 2254–2264 https://doi.org/10.2337/db14-1220

59 Cotte, A. K., Cottet, V., Aires, V., Mouillot, T., Rizk, M., Vinault, S., et al. (2019) Phospholipid profiles and hepatocellular carcinoma risk and prognosis in cirrhotic patients. *Oncotarget* **10**, 2161–2172 https://doi.org/10.18632/oncotarget.26738

**Legends:**

Fig. 1: Lipid affinity test of Lo18. Immunolabeling measurements were performed on Lo18 and several common phospholipids: unsaturated (dioleoyl, DO-) or saturated (dipalmitoyl, DP-) lipids with neutral (phosphatidylethanolamine, -PE and phosphatidylcholine, -PC) or negative (phosphatidic acid, -PA and phosphatidylglycerol, -PG) charged head groups. The intensity of the signal obtained after hybridization with Lo18 was normalized with the number of phospholipids fixed to the PVDF membrane. The data represent the means and SE of three independent experiments and were analyzed statistically by the Kruskal-Wallis nonparametric test.

Fig. 2: Lipidic composition of the liposomes used. Lipidic profiles of (i) *O. oeni* liposomes in exponential, stationary, or 36 h ethanol-adapted culture, or (ii) *L. plantarum* liposomes. Proportion of polar head group type (A) and fatty acids (B) of each liposome. The data represent the means and SE of three independent experiments and were analyzed statistically by Kruskal-Wallis nonparametric test.

Fig. 3: Lipochaperone activity of Lo18 according to the lipidic substrate. Measure of fluorescence anisotropy of DPH inserted into liposomes of: (i) *O. oeni* in the exponential phase (circle), the stationary phase (square), or 36 h ethanol-adapted culture (inverted triangle), or (ii) L. *plantarum* liposomes (triangle) during thermal ramping between 15 to 60°C in the absence (white symbols) or presence of Lo18 (colored symbols). The data represent the means and SE of three independent experiments and were analyzed statistically by the Mann-Whitney U-test.

Fig. 4: Secondary structure modification of Lo18 in interaction with liposomes of –i) *O. oeni* in exponential phase, stationary phase or 36h ethanol-adapted culture or (ii) *L. plantarum* liposomes. Proportion of secondary structure, α-helix and β-sheet (A) SRCD spectra on 190-240 nm wavelength at 15 °C (B) and 45°C (C) of Lo18 alone (black) or in the presence of liposomes from *O. oeni culture* in exponential phase (purple), stationary phase (blue) or 36h ethanol-adapted culture (turquoise) and *L. plantarum* culture (orange) (A). The data represent the means and SE of three independent experiments and were analyzed statistically by Kruskal-Wallis nonparametric test, $pV < 0.05$.

Fig. 5: Part of the mechanisms by which membrane lipids interact with Lo18. Summary table of influence of lipid environment and physiological state of membranes on lipochaperone activity, secondary structure, interaction and insertion of Lo18 with membrane (A). Schematic illustration of Lo18-membrane interaction (B). During an association/dissociation cycle of Lo18 oligomeric subunits, the protein may be attracted to the membrane by electrostatic and/or hydrophobic forces, allowing the protein to chaperone and/or insert into the membrane.

Supplementary data, table S1: Lipidomic analysis of the four liposomes used during the experiments. Data corresponding to means ± SE and statistical analysis for each line. Measurements were replicated three times and analyzed by Kruskal-Wallis statistical test (P-value<0.05).

652 Supplementary data, table S2: Anisotropy measurement of liposomes of (i) *O. oeni* in the
653 exponential phase and stationary phase, or in ethanol-adapted culture or (ii) *L. plantarum* culture
654 during thermal ramping between 15 to 65 °C in the absence or presence of Lo18. The data present
655 the means of three independent experiments.
656
657 Supplementary data, Fig. S1: Lipid staining by 50 mM of Nile Red of several common
658 phospholipids: unsaturated (dioleoyl, DO-) or saturated (dipalmitoyl, DP-) lipids with neutral
659 (phosphatidylethanolamine, -PE and phosphatidylcholine, -PC) or negative (phosphatidic acid, -
660 PA and phosphatidylglycerol, -PG) charged head group (A). Immunolabeling interaction between
661 Lo18 and several common phospholipids (B). The membrane presented corresponds to an
662 experiment representative of three independent measurements.
663

Figure 1

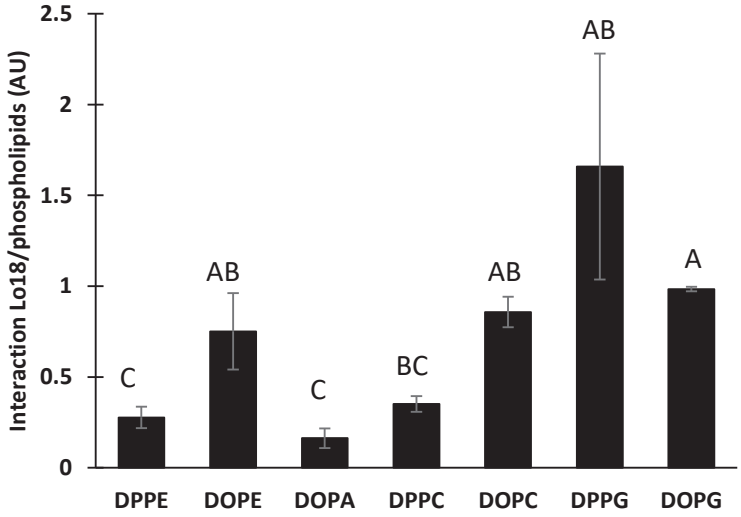
Interaction Lo18/phospholipids (AU)
2.5
2
1.5
1
0.5
0
C
AB
C
BC
AB
AB
A
DPPE
DOPE
DOPA
DPPC
DOPC
DPPG
DOPG

Figure 2

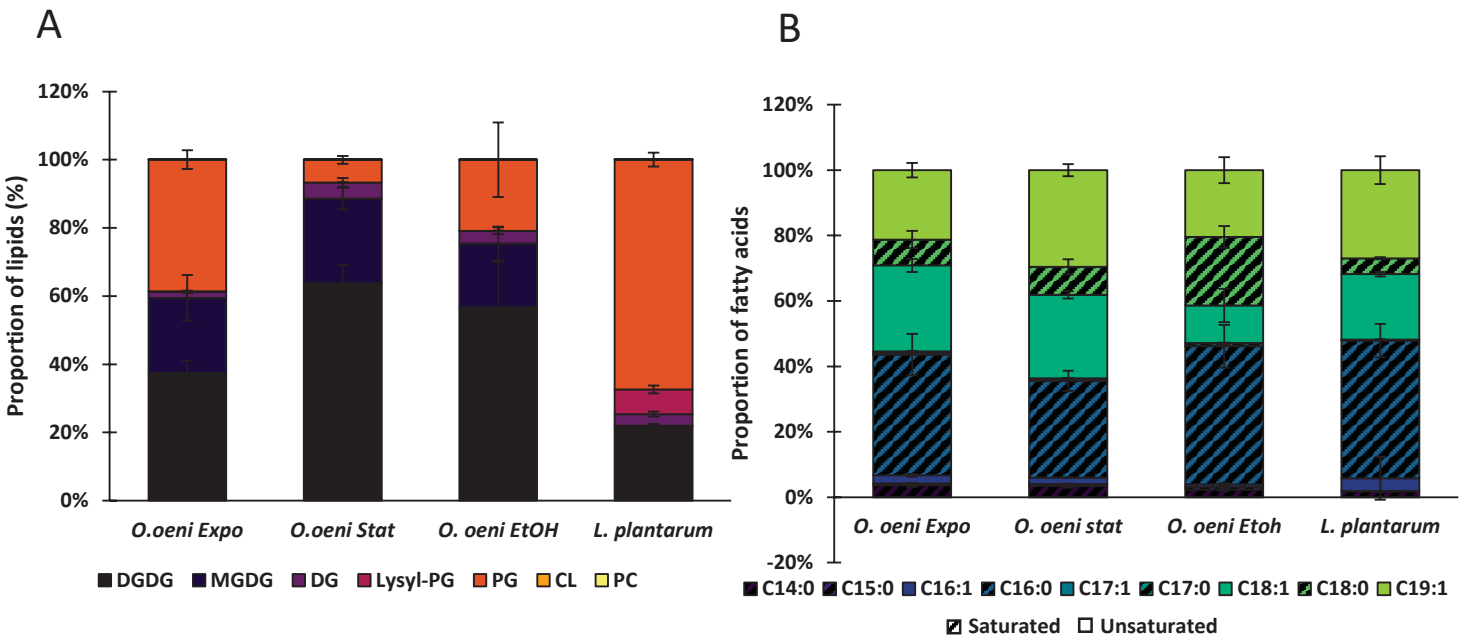
A
120%
100%
80%
60%
40%
20%
0%
Proportion of lipids (%)
O.oeni Expo
O.oeni Stat
O. oeni EtOH
L. plantarum
DGDG
MGDG
DG
Lysyl-PG
PG
CL
PC
B
120%
100%
80%
60%
40%
20%
0%
-20%
Proportion of fatty acids
O. oeni Expo
O. oeni stat
O. oeni Etoh
L. plantarum
C14:0
C15:0
C16:1
C16:0
C17:1
C17:0
C18:1
C18:0
C19:1
Saturated
Unsaturated

Figure 3

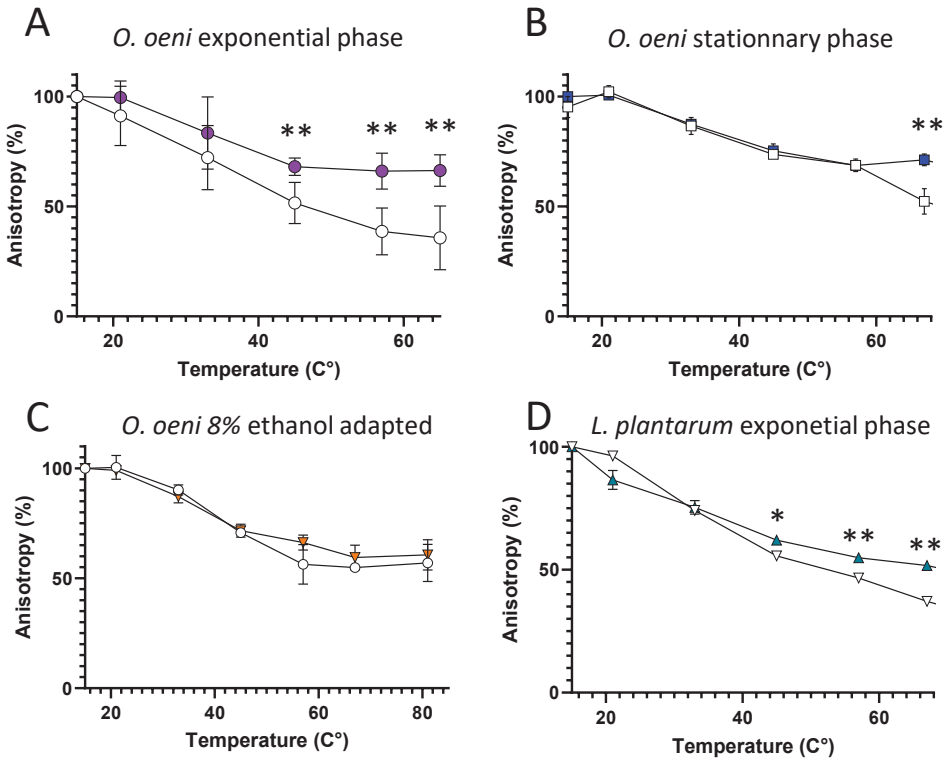
A
O. oeni exponential phase
B
O. oeni stationnary phase
C
O. oeni 8% ethanol adapted
D
L. plantarum exponetial phase
Anisotropy (%)
Temperature (C°)
100
50
0
20
40
60
80
*
**

Figure 4

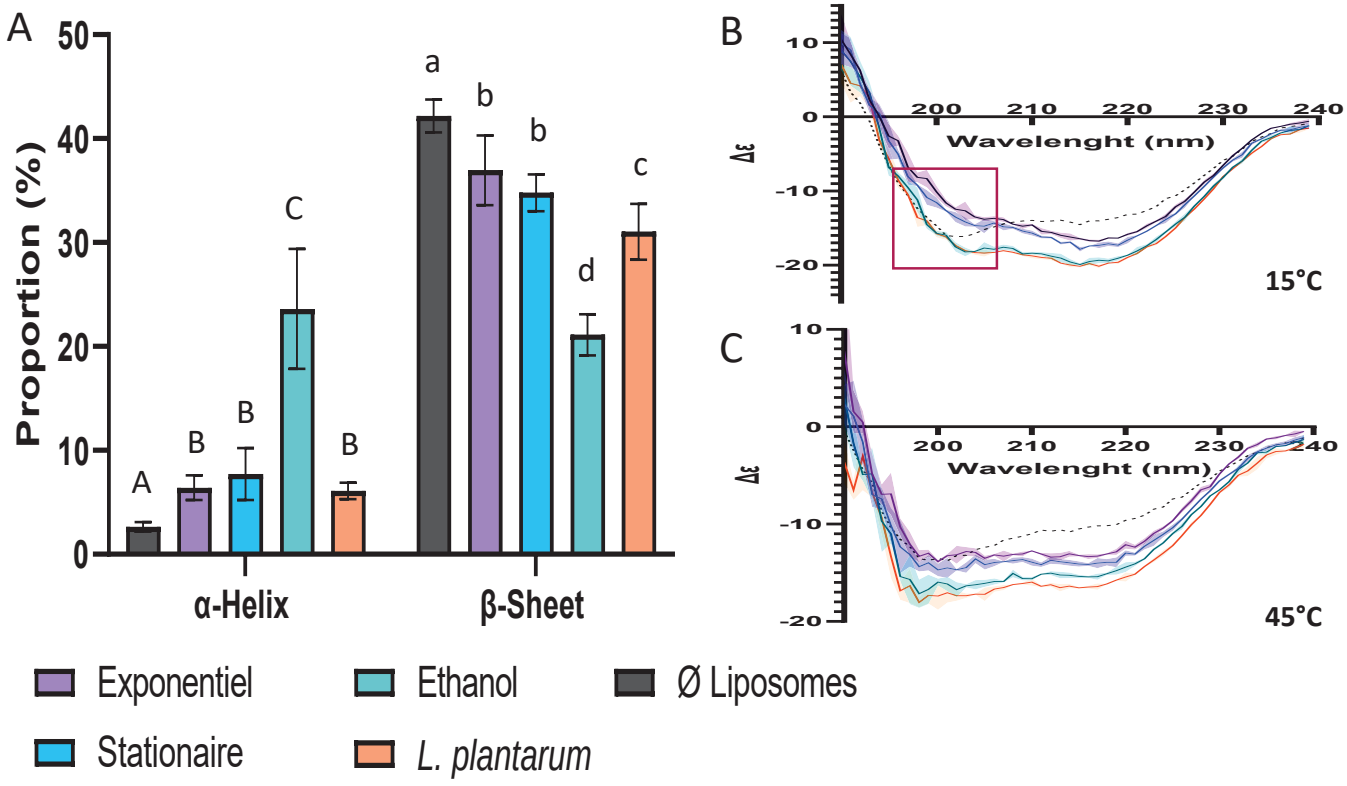
A
Proportion (%)
50
40
30
20
10
0
A
B
B
C
B
a
b
b
d
c
α-Helix
β-Sheet
B
10
0
-10
-20
200
210
220
230
240
Wavelenght (nm)
Δε
15°C
C
10
0
-10
-20
200
210
220
230
240
Wavelenght (nm)
Δε
45°C
Exponentiel
Stationaire
Ethanol
L. plantarum
Ø Liposomes

Figure 5

A

| Microorganisms | | *O. oeni* | | *L. plantarum* |
|---|---|---|---|---|
| Growth phase | Exponential | Stationary | Ethanol-adapted | Exponential |
| Lipids composition | PG+;DO+ | PG-;DO+ | PG-;DO- | PG+;DO- |
| Lipochaperon activity | ++ | +/- | - | ++ |
| Protein structures change (α;β) | +;- | +;- | ++;--- | +;-- |
| Insertion | + | + | - | - |

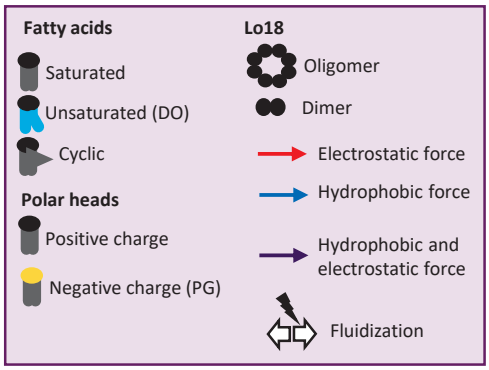


B

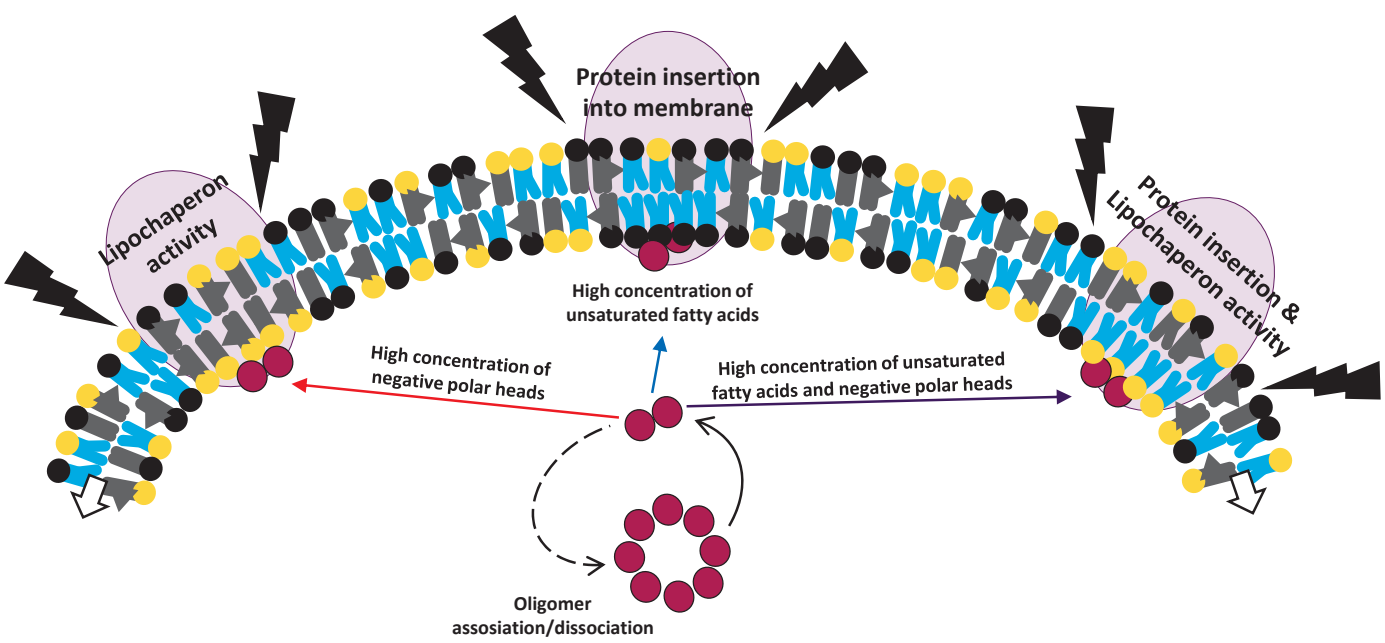

Supplementary data, Table S1

| | | *O. oeni* Exponential | *O. oeni* Stationary | *O. oeni* Ethanol 8% | *L. plantarum* |
|---|---|---|---|---|---|
| Fatty acids (%) | **C14:0** | 3.7 ± 0.5 A | 3.5 ± 0.5 A | 2.3 ± 0.4 AB | 1.8 ± 0.2 B |
| | **C15:0** | 0.6 ± 0.1 A | 0.5 ± 0.1 A | 0.8 ± 0.1 A | 0.1 ± 0 B |
| | **C16:1** | 2.4 ± 0.6 A | 1.9 ± 0.5 A | 0.8 ± 0.3 A | 3.9 ± 0.8 B |
| | **C16:0** | 36.9 ± 6.3 A | 29.6 ± 3.1 A | 42.2 ± 6.5 A | 42.1 ± 5.1 A |
| | **C17:1** | 0.6 ± 0.1 A | 0.4 ± 0.1 AB | 0.3 ± 0.1 BC | 0.2 ± 0.1 C |
| | **C17:0** | 0.4 ± 0.1 B | 0.4 ± 0.1 B | 0.7 ± 0.1 A | 0.1 ± 0 C |
| | **C18:1** | 26.3 ± 2 A | 25.5 ± 1.1 A | 11.5 ± 5.1 B | 20 ± 0.7 B |
| | **C18:0** | 7.9 ± 2.7 A | 8.6 ± 2.3 A | 21 ± 3.3 B | 4.9 ± 0.3 A |
| | **C19:1** | 21.2 ± 2.2 A | 29.6 ± 1.9 A | 20.4 ± 3.9 A | 26.9 ± 4.2 A |
| Polar head groups (%) | **DGDG** | 37.5 ± 33.5 AB | 63.8 ± 5.3 A | 56.7 ± 13.3 A | 21.6 ± 0.9 B |
| | **MGDG** | 22 ± 6.7 A | 24.8 ± 3.2 A | 18.7 ± 4.9 A | 0.3 ± 0.1 B |
| | **DG** | 1.7 ± 0.3 A | 4.7 ± 1.3 A | 3.7 ± 1.1 A | 3.4 ± 0.7 A |
| | **Lysyl-PG** | 0.2 ± 0.2 A | 0 ± 0 A | 0 ± 0 A | 7.2 ± 1.1 B |
| | **PG** | 38.6 ± 2.7 AB | 6.7 ± 1.2 C | 20.8 ± 10.9 BC | 67.4 ± 2 A |
| | **CL** | 0.009 ± 0.003 A | 0.05 ± 0.01 B | 0.02 ± 0.008 AB | 0.002 ± 0.0005 C |
| | **PC** | 0.0001 ± 0.00008 A | 0.00006 ± 0.000004 A | 0.0003 ± 0.0002 A | 0.0007 ± 0.0001 B |

Supplementary data, Table S2

| | | *O. oeni* | | | *L. plantarum* |
|---|---|---|---|---|---|
| | **Condition** | **Exponential** | **Stationary** | **Ethanol-adapted** | **Exponential** |
| **Anisotropy without Lo18** | **15°C** | 0.189 | 0.185 | 0.201 | 0.186 |
| | **65°C** | 0.070 | 0.105 | 0.108 | 0.070 |
| | **Rate of fluidification (%)** | -63.0 | -43.4 | -46.2 | -62.3 |
| | **Slope** | -0.0024 | -0.0016 | -0.0019 | -0.0023 |
| **Anisotropy with Lo18** | **15°C** | 0.220 | 0.228 | 0.239 | 0.208 |
| | **65°C** | 0.155 | 0.161 | 0.144 | 0.103 |
| | **Rate of fluidification (%)** | -29.5 | -29.2 | -39.8 | -50.5 |
| | **Slope** | -0.0013 | -0.0013 | -0.0019 | -0.0021 |

Supplementary data, Figure S1

A

Nil Red coloration control

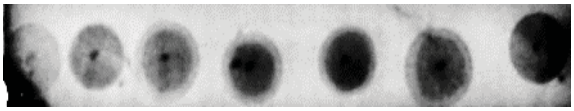

DPPE DOPE DOPA DPPC DOPC DPPG DOPG

B

Immunostaining

Supplementary data, Table S1

| | | *O. oeni* Exponential | *O. oeni* Stationary | *O. oeni* Ethanol 8% | *L. plantarum* |
|---|---|---|---|---|---|
| Fatty acids (%) | **C14:0** | 3.7 ± 0.5 A | 3.5 ± 0.5 A | 2.3 ± 0.4 AB | 1.8 ± 0.2 B |
| | **C15:0** | 0.6 ± 0.1 A | 0.5 ± 0.1 A | 0.8 ± 0.1 A | 0.1 ± 0 B |
| | **C16:1** | 2.4 ± 0.6 A | 1.9 ± 0.5 A | 0.8 ± 0.3 A | 3.9 ± 0.8 B |
| | **C16:0** | 36.9 ± 6.3 A | 29.6 ± 3.1 A | 42.2 ± 6.5 A | 42.1 ± 5.1 A |
| | **C17:1** | 0.6 ± 0.1 A | 0.4 ± 0.1 AB | 0.3 ± 0.1 BC | 0.2 ± 0.1 C |
| | **C17:0** | 0.4 ± 0.1 B | 0.4 ± 0.1 B | 0.7 ± 0.1 A | 0.1 ± 0 C |
| | **C18:1** | 26.3 ± 2 A | 25.5 ± 1.1 A | 11.5 ± 5.1 B | 20 ± 0.7 B |
| | **C18:0** | 7.9 ± 2.7 A | 8.6 ± 2.3 A | 21 ± 3.3 B | 4.9 ± 0.3 A |
| | **C19:1** | 21.2 ± 2.2 A | 29.6 ± 1.9 A | 20.4 ± 3.9 A | 26.9 ± 4.2 A |
| Polar head groups (%) | **DGDG** | 37.5 ± 33.5 AB | 63.8 ± 5.3 A | 56.7 ± 13.3 A | 21.6 ± 0.9 B |
| | **MGDG** | 22 ± 6.7 A | 24.8 ± 3.2 A | 18.7 ± 4.9 A | 0.3 ± 0.1 B |
| | **DG** | 1.7 ± 0.3 A | 4.7 ± 1.3 A | 3.7 ± 1.1 A | 3.4 ± 0.7 A |
| | **Lysyl-PG** | 0.2 ± 0.2 A | 0 ± 0 A | 0 ± 0 A | 7.2 ± 1.1 B |
| | **PG** | 38.6 ± 2.7 AB | 6.7 ± 1.2 C | 20.8 ± 10.9 BC | 67.4 ± 2 A |
| | **CL** | 0.009 ± 0.003 A | 0.05 ± 0.01 B | 0.02 ± 0.008 AB | 0.002 ± 0.0005 C |
| | **PC** | 0.0001 ± 0.00008 A | 0.00006 ± 0.000004 A | 0.0003 ± 0.0002 A | 0.0007 ± 0.0001 B |

Supplementary data, Table S2

| | | *O. oeni* | | | *L. plantarum* |
|---|---|---|---|---|---|
| | **Condition** | **Exponential** | **Stationary** | **Ethanol-adapted** | **Exponential** |
| **Anisotropy without Lo18** | **15°C** | 0.189 | 0.185 | 0.201 | 0.186 |
| | **65°C** | 0.070 | 0.105 | 0.108 | 0.070 |
| | **Rate of fluidification (%)** | -63.0 | -43.4 | -46.2 | -62.3 |
| | **Slope** | -0.0024 | -0.0016 | -0.0019 | -0.0023 |
| **Anisotropy with Lo18** | **15°C** | 0.220 | 0.228 | 0.239 | 0.208 |
| | **65°C** | 0.155 | 0.161 | 0.144 | 0.103 |
| | **Rate of fluidification (%)** | -29.5 | -29.2 | -39.8 | -50.5 |
| | **Slope** | -0.0013 | -0.0013 | -0.0019 | -0.0021 |

Supplementary data, Figure S1

A

Nil Red coloration control

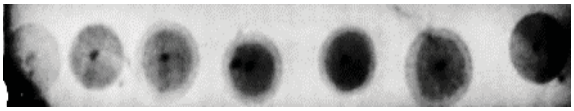

DPPE DOPE DOPA DPPC DOPC DPPG DOPG

B

Immunostaining